Published in final edited form as:
Lancet Neurol. 2011 September ; 10(9): 785–796. doi:10.1016/S1474-4422(11)70156-9.

Neuropathologically defined subtypes of Alzheimer's disease with distinct clinical characteristics: A retrospective study

Melissa E. Murray, PhD[1], **Neill R. Graff-Radford, MBBCh, FRCP (London)**[3], **Owen A. Ross, PhD**[1], **Ronald C. Petersen, MD**[4], **Ranjan Duara, MD**[5], and **Dennis W. Dickson, MD**[1]

[1]Department of Neuroscience, Mayo Clinic, Jacksonville, Florida.

[3]Department of Neurology, Mayo Clinic, Jacksonville, Florida.

[4]Department of Neurology, Mayo Clinic, Rochester, Minnesota.

[5]Wien Center for Alzheimer's Disease and Memory Disorders, Mount Sinai Medical Center, Miami Beach, and Miller School of Medicine, University of Miami

Abstract

Objective—Neurofibrillary pathology has a stereotypic progression in Alzheimer's disease (AD) that is encapsulated in the Braak staging scheme. Some AD cases do not fit the Braak staging scheme and are considered atypical. The purpose of this study was to compare clinical and pathological features of typical AD with atypical AD that had either hippocampal sparing (HpSp) and limbic-predominant (LP) neurofibrillary pathology.

Correspondence to: Dennis W. Dickson, M.D. Robert E. Jacoby Professor of Alzheimer's Research Mayo Clinic 4500 San Pablo Road Jacksonville, FL 32224 Phone: 904-953-7137 Fax: 904-953-7117 dickson.dennis@mayo.edu.

Ethical approval:
All research reported is on postmortem material, which is considered exempt from human subject research. All brains were acquired with appropriate ethical approval and research described has approval from the Mayo Clinic Institutional Review Board.

Role of funding source
The funding sources had no role in study design, collection, analysis, interpretation, or decision to submit this paper.

Contributors
With the guidance of DWD, NRG, OAR, and RD in conception and design, MEM was primarily responsible for algorithm development of AD types and digital microscopy quantification. DWD conducted NFT acquisition, as well as pathologic diagnoses. NRG, RD and RCP guided clinical data extraction from patient reports. OAR was responsible for acquisition of genetic data. MEM was responsible for acquisition of data and statistical analysis. Interpretation of data was performed by all authors. MEM drafted the original manuscript, which was revised by DWD, NRG, OAR, and RD. Final manuscript approval was granted by all authors.

Conflicts of Interest
The authors have nothing to disclose.

Systematic review
We searched PubMed for articles published in English with the search terms hippocampal sparing Alzheimer's disease (AD), atypical AD, hippocampus, disease duration and neurofibrillary tangles, tangle predominant dementia, tau spread and AD, and AD biomarkers to identify the current understanding of atypical AD. The publishing dates for PubMed literature search was for the years 1984 – 2011.

Interpretation
Previous studies have reported an atypical variant of AD, but have lacked pathologic verification of clinical findings. We have identified two distinct clinicopathologic subtypes of AD (hippocampal sparing and limbic predominant) using quantitative data to stratify atypical from typical AD in pathologically-confirmed cases. The increased rate of cognitive decline in hippocampal sparing AD suggests that neurofibrillary pathology in the primary cortices has a greater influence on MMSE scores than hippocampal pathology. *MAPT* and *APOE* findings support evidence of a genetic influence on AD subtypes. These findings should be considered with age of onset and non-AD clinical presentation in the differential diagnosis of atypical AD.

Methods—A mathematical algorithm was devised to classify AD cases into typical, HpSp and LP according to the density and distribution of neurofibrillary tangle (NFT) counts from thioflavin S fluorescent microscopy in three cortical regions and two Hp sectors. The algorithm was applied to NFT counts of 889 cases of AD (409 men and 480 women; age at death: 37-103 years). Cases so classified were compared on clinical, demographic, pathological and genetic grounds. An independent series of 113 cases of AD were similarly evaluated to validate findings from the initial cohort.

Findings—In comparison to typical AD, HpSp (n=97) had higher NFT densities in cortical areas and lower NFT densities in hippocampus, while LP (n=127) had lower NFT densities in cortical areas and higher NFT densities in the Hp. HpSp had less Hp atrophy than typical AD (11%) and LP (14%). HpSp were younger, with a higher proportion of men, whereas LP was older, with a higher proportion of women. *MAPT* H1H1 genotype was more frequent in LP compared with HpSp, but not between LP and typical AD. *APOE* ε4 allele status differed among AD subtypes only when age of onset was considered. Clinical presentation, age of onset, disease duration, and rate of decline differed among the AD subtypes. The findings were confirmed in a replication cohort.

Interpretation—Our data supports the hypothesis of distinct clinicopathologic subtypes of AD. HpSp and LP AD account for about 25% of AD and are important to consider in clinical, genetic, biomarker and treatment studies.

Keywords

Alzheimer disease; APOE; digital microscopy; hippocampus; MAPT; neurofibrillary tangles; thioflavin S fluorescent microscopy

Introduction

Hippocampal atrophy rates have been used as a biomarker to track progression of Alzheimer's disease (AD) and to predict cognitive decline.[1-5] On the other hand, a subset of AD cases has been observed to have hippocampal sparing (HpSp) relative to the degree of cortical atrophy.[6] These cases challenge current concepts of disease progression in AD as encapsulated in the Braak and Braak staging scheme of neurofibrillary changes.[7]

Neurofibrillary tangles (NFTs) and senile plaques (SPs) are the characteristic structural lesions assessed in neuropathologic diagnosis of AD.[8] Their spatial pattern is considered predictable;[7, 9] however, variability can be found in neuroimaging and neuropathology studies.[1, 2, 6, 10-13] An early report evaluating interhemispheric asymmetry noted one case with sparing of the hippocampus relative to the widespread cortical degeneration.[6] A later report demonstrated more severe pathology in occipital-parietal cortices relative to frontal and temporal cortices in a subset of AD presenting with posterior cortical atrophy.[12] These observations, although from small case series, suggest that there may not be a single pattern of pathological progression of neurofibrillary degeneration in AD, with its origin in the transentorhinal cortex, progressing through the hippocampus to eventually target association and finally primary cortices.[7] In previous studies from our laboratory, we noted a subset of AD cases, usually in the setting of Lewy body disease, that had relative sparing of the hippocampus (HpSp) from neurofibrillary pathology,[14] but the frequency and clinical significance of this subtype of AD has not been previously explored. In contradistinction to HpSp are cases of AD with severe and relatively restricted medial temporal NFT,[15] which we refer to as limbic predominant (LP) AD. The frequency and clinical implications of atypical AD have been neglected in research on large autopsies series. The purpose of this study was to develop an operational classification method to separate typical and atypical AD based upon counts of NFT in hippocampus and cortex and to determine clinical,

pathological and genetic implications of the subtypes of AD in a large (n=889) consecutive series of pathologically confirmed AD cases. To this end, we studied differences in NFT and SP density in regions not used in the classification algorithm; structural differences in the hippocampus and entorhinal cortex with digital microscopy methods; clinical differences in terms of clinical diagnosis and disease progression; and genetic differences with respect to microtubule-associated protein tau (*MAPT*) and apolipoprotein E (*APOE)* genotypes. Finally, we studied these same factors in an independent replication cohort of 113 AD patients derived from a single center from a community-based prospective longitudinal study.

Subjects and Methods

Case Material

The brain bank database at the Mayo Clinic Jacksonville was queried for AD cases with a Braak NFT stage >IV, absence of hippocampal sclerosis, presence of data on NFT counts with thioflavin-S fluorescent microscopy, and presence of paraffin blocks for further studies (n = 889; 409 men and 480 women; age at death: 37-103 years). The AD cases were mostly from two sources - the State of Florida Alzheimer's Disease Initiative (ADI) (n = 589; 66%) and the Mayo Clinic Jacksonville Memory Disorder Clinic (n = 155; 17%). The remaining cases were from a variety of referral sources (n = 144), including 21 (2%) from Einstein Aging Study (P01 AG03949), 29 (3%) from the Society of Progressive Supranuclear Palsy, 22 (2%) from Mayo Clinic Jacksonville Movement Disorder Clinic, 8 (1%) from the Florida Alzheimer's Disease Research Center (P50 AG25711), and 65 (7%) from various referring hospitals. The ADI is a Florida Department of Elder Affairs-supported program that provides autopsy confirmation for patients who completed at least one visit to one of the memory disorder clinics located across the state.[16] The clinical information is obtained at enrollment. The ADI is not a longitudinal study; however, standardized longitudinal clinical information is collected on a subset of ADI patients evaluated at the Wien Center for Alzheimer's Disease and Memory Disorders, Mount Sinai Medical Center, Miami Beach, FL, and from patients followed at the Mayo Clinic Jacksonville Memory Disorder Clinic. Differences with respect to study source are reported in **Supplemental Tables 1-4**.

All cases underwent standardized neuropathologic assessment by a single neuropathologist (DWD), which included gross and microscopic evaluation. Using thioflavin-S fluorescent microscopy, quantitative measures of SP and NFT densities were assessed with an Olympus BH2 fluorescent microscope and a Braak NFT stage assigned as previously described based upon the distribution of NFTs (**Figure 1**).[17-19] The neuroanatomical sampling design and procedures for thioflavin S fluorescent microscopy used in this study were developed originally by Dr. Robert D. Terry.[19] SP counts included total counts - primitive, neuritic and cored type plaques. In this study, no effort was made to differentiate SP subtypes. The count was truncated at 50, which is more than twice the number required for neuropathologic diagnosis of AD using the Khatchaturian criteria.[20] NFT counts, including intracellular and extracellular tangles, from two sectors of the hippocampus (CA1 and subiculum) and three association cortices (mid-frontal, inferior parietal, and superior temporal), were used to classify typical and atypical AD according to a mathematical algorithm (see below). Additional areas with NFT counts not included in the algorithm were the lateral and medial amygdala, CA2/3 sector and endplate of the hippocampus, as well as the primary motor and visual cortices. At the time of pathologic diagnosis, family history of neurodegenerative disease was noted and recorded in the database as present or absent. Cerebrovascular disease was assessed using a simple scheme proposed by Jellinger and Atterns,[21] as previously reported.[22] TAR DNA binding protein 43 (TDP-43) pathology[23] and Lewy body pathology[17] were assessed with immunohistochemistry as previously described. The frequency of non-Alzheimer pathologies is reported in **Table 1**.

All research reported is on postmortem material, which is considered exempt from human subject research. All brains were acquired with appropriate ethical approval, and the research described has approval from the Mayo Clinic Institutional Review Board.

Validation series—An independent cohort of 113 cases of AD that met similar inclusion and exclusion criteria as the discovery set were processed for thioflavin S fluorescent microscopy as described above. They were almost all derived from a community-based cohort, the Alzheimer's Disease Patient Registry (ADPR; U01 AG06786), which recruits patients from primary care clinics at Mayo Clinic in Rochester, MN. Subtypes of AD were classified based upon NFT counts from the classification algorithm, and then compared to the discovery cohort with respect to clinical, pathological and genetic characteristics (see **Supplemental Table 5**). The operational classification was also compared to neuropathologic diagnosis of HpSp or LP AD as recorded at the time of diagnostic evaluation (see **Supplemental Table 6**).

Operational classification of AD variants

To objectively classify AD cases into typical and atypical, including HpSp and LP types, a logical function was designed in Microsoft Excel (Redmond, WA). The steps used in this algorithm and the portioning of cases at each step are illustrated in **Figure 2**. Three requirements were written into the algorithm to return HpSp: 1) the ratio of the average hippocampal NFT to the average cortical NFT had to be less than the 25th percentile of all AD cases (ratio = 1.1), 2) all three of the hippocampal NFT densities [CA1 (median = 12), subiculum (median = 20), CA1-subiculum average (median = 17)] had to be less than the median values, and 3) at least three of the cortical NFT measures [superior temporal (median = 10), inferior parietal (median = 8), mid-frontal (median = 5), and cortical average (median = 8)] had to be greater than or equal to the median values. A separate logical function was written for LP, which reversed the signs and set a higher threshold for the NFT ratio: 1) the ratio of the average hippocampal NFT to the average cortical NFT had to be greater than the 75th percentile of all AD cases (ratio = 3.6) 2) all three of the hippocampal NFT densities had to be greater than the median values, and 3) at least three of the cortical NFT measures had to be less than or equal to the median values. The cases not designated either HpSp (n=97) or LP (n=127) were considered to be typical AD (n=665) (**Table 1**).

The use of median values enabled the algorithm to offset over/underestimating differences between regions. For example, it was not uncommon for a Braak NFT stage V case to have none-to-sparse NFTs in the middle frontal gyrus, while in the same case the superior temporal and inferior parietal cortices would have many NFTs. The use of the hippocampal-to-cortical ratio prevented AD cases with overall mild neurofibrillary pathology from being incorrectly classified as HpSp.

Clinical history

Antemortem clinical information was gathered from clinic reports blinded to AD type. Given the large number of case reports and the absence of standardized longitudinal data on many of the cases, the entire AD sample (n=889) was not screened for clinical information. Instead, all HpSp (n=97) and LP (n=127) cases were evaluated, as well as twice the number of typical AD (n=232) cases. The age of onset, education, and Mini-mental state exam (MMSE)[24] scores were the parameters recorded. Clinical data were available on a subset of HpSp, typical and LP AD, respectively [age of onset: n=73 (75%), n=203 (86%), n=77 (61%); education: n=71 (73%), n=214 (92%), n=90 (71%); MMSE (>1 testing visit): n=43 (44%), n=160 (69%), n=46 (36%); and longitudinal MMSE (>3 testing visit): n=18 (20%), n=52 (22%), n=18 (14%)]. Disease duration and elapsed time between MMSE test date was calculated by subtracting either date of onset or MMSE test date from date of death and

dividing by 364.25 (*i.e.* time in years). Longitudinal decline was calculated for any case with three or more MMSE testing dates and scores using the Excel SLOPE function. The MMSE score was the dependent variable and the elapsed time between testing and death was the independent variable. The slope was calculated anywhere along the disease trajectory that MMSE data was available, regardless of perimortem tests unless the subject was untestable and scored as a 0. The median longitudinal decline for each AD type is reported in **Table 1**.

Digital Microscopy

Five-micrometer thick sections of formalin-fixed, paraffin-embedded tissue from the posterior hippocampus at the level of the lateral geniculate were stained with hematoxylin and eosin (H&E) for structural analysis. The slides were scanned on the ScanScope XT (Aperio, Vista, CA) at 20x and annotated using ImageScope v10.2 software (Aperio, Vista, CA). Anatomic criteria for hippocampal sectors was based on the work of Duvernoy.[25]

Hippocampal area—The lateral border was the temporal horn, and the inferior border was the white matter of the parahippocampal gyrus. The fimbria was not included in the overall area measure (**Supplemental Figure 1**). The hippocampal area was normalized to the fixed brain weight for each case (mm^2/g).

CA1-subiculum—This region included the pyramidal cell layer at the CA1-subiculum border. A ruler tool was used to measure the thickness in triplicate to account for variations between CA1-subiclum. This same region was annotated for the analysis of neuronal density (**Supplemental Figure 1**). Neuronal density was quantified by dividing the number of neurons with the annotated area ($neurons/mm^2$).

CA1-subliculum/Fusiform—The fusiform gyrus was measured in triplicate along the section of the gyrus parallel to the pial surface. A ratio was calculated between the hippocampal and cortical thickness measures to determine hippocampal atrophy relative to cortical thickness. The hippocampal thickness included two layers (pyramidal and lacunosum), whereas the cortical thickness included all six; therefore, a ratio equal to 1.00 was not expected. A higher ratio is interpreted as a thicker CA1-subiculum relative to the fusiform gyrus. Conversely, a smaller ratio is interpreted as a thinner CA1-subiculum relative to the fusiform gyrus.

Neuron count—The Nuclear v9 macro template (Aperio, Vista, CA) was modified to detect pyramidal neurons in the CA1 and subiculum of the hippocampus on H&E. Default settings were adjusted to accommodate the range in shapes, sizes, and cytoplasmic intensities. The segmentation was changed to Nuclear stain to enable detection of the basophilic properties of the nucleus and cytoplasm. The amplitude threshold was selected to calculate upper and lower values based on the inherent statistical analysis of pixel values. The minimum nuclear size was increased to avoid erroneous selection of hypertrophic astrocytes. Minimum roundness was increased to ignore astrocytes being falsely counted. On a subset of cases the neurons were manually counted using ImageScope (Aperio, Vista, CA) 20x window. A 6.8% error rate was found when the manual counts were compared to the neuronal counts generated by the custom-designed algorithm.

Genotyping of AD cases

MAPT and *APOE* genotyping was available on 472 AD cases (272 women and 200 men; age range, 57-102 years; mean age, 79 years). Of the total 472 genotyped cases, 52 were classified as HpSp, 343 as typical AD, and 77 as LP. DNA was obtained from frozen brain tissue using standard protocols. Each sample was genotyped for *MAPT* H1/H2 (SNP rs1052553 A/G, A=H1, G=H2) and *APOE*, and the *SNCA* 3'UTR SNP rs356165.

Genotyping for a risk variant in the gene for α-synuclein [*SNCA*, 3'UTR SNP rs356165 (G/A)], was available on 438 cases (353 women and 186 men; age range, 55-102 years; mean age, 79 years). Frozen brain tissue was used to extract genomic DNA according to methods described previously.[26-28] *MAPT* and *SNCA* genotypes were determined using a Sequenom MassArray iPLEX platform (Sequenom, San Diego, CA) and analyzed with Typer 4.0 software (also from Sequenom). The *APOE* genotype was determined using TaqMan chemistry. Cases with genotype data were similar to the total cohort with respect to AD subtype (*MAPT and APOE:* HpSp = 54%, Typical = 52%, LP = 61%; *SNCA*: HpSp = 52%, Typical = 48%, LP = 54%).

Statistical Methods

All statistical data and graphs were analyzed using SigmaPlot (Ver 11, San Jose, CA). The difference in mean values of continuous data was determined using Analysis of Variance (ANOVA) tests with post-hoc pairwise comparisons run using a t-test. Analysis of categorical data used a Chi-square to determine whether the proportions of observations varied between the AD types. A Kruskal-Wallis One Way Analysis of Variance on Ranks was used on all quantitative pathologic data and MMSE test differences. Pairwise comparisons between AD types were tested with the Mann-Whitney rank sum. Three Multiple Logistic Regression models were constructed to control for coexisting Lewy body diagnosis affected the *MAPT* result (*i.e.* independent variables) amongst the AD subtypes (*i.e.* dependent variables). Spearman Rank Order correlation was used to determine the relationship between both neuronal density or NFT density and clinical measures of disease duration and age of onset.

Results

Initial cohort

The demographic, pathologic, and clinical information of typical and atypical AD cases are summarized in **Table 1**. Of the 889 AD cases that met study criteria, 11% were operationally classified as HpSp based on the sparse distribution of NFT in the hippocampus (median = 8) compared to the three association cortices (median = 13) and a hippocampal:cortical ratio within the first quartile. Of the remaining AD cases, 14% were classified as LP based on high density of NFT in the hippocampus (median = 27) and much less in the cortical regions (median = 4) and a hippocampal:cortical ratio within the last quartile. The reason that there are fewer HpSp (n = 97) than LP cases (n = 127) is a result of the difference in median NFT densities in the hippocampal (*i.e.* CA1 and subiculum) and cortical areas (*i.e.* superior temporal, inferior parietal, and middle frontal) individually evaluated (see **Figure 2**).

HpSp cases were younger at death and had a higher male:female ratio compared to the other two types. The LP cases were older at death and had a lower male:female ratio compared to the other two types. There were no differences in fixed brain weight or Braak NFT stage between typical and atypical AD (Table 1). There was less frequent TDP-43, cerebrovascular and Lewy body pathologies in HpSp than in both LP and typical AD, but there were no differences between LP and typical AD with respect to these non-Alzheimer type pathologies.

Table 2 shows the results of pathologic and structural comparisons between typical and atypical AD. HpSp cases had lower hippocampal NFT counts than both LP and typical AD (**Figure 3**). Unexpectedly, the three association cortices had higher NFT counts in HpSp compared with LP and typical AD. Conversely, LP had lower cortical NFT and higher hippocampal NFT than both HpSp and typical AD. Hippocampal sectors less vulnerable to

NFT pathology (*i.e.* CA2/3, endplate), which were not included in the classification algorithm, both showed lower NFT counts in HpSp and higher NFT counts in LP. The visual and motor cortices, which have low NFT counts in most AD cases and were not included in the classification algorithm, were also studied. The NFT counts in visual cortex showed no differences between AD types, but the primary motor cortex had higher NFT counts in HpSp. The NFT in amygdala, which were not included in the classification algorithm, were higher in LP than HpSp and typical AD. NFT counts were highest in the medial aspect of the amygdala compared to the basolateral region. There were no significant differences across the AD subtypes with respect to SP counts in the three association cortices. Of the hippocampal SP counts, only the CA2/3 showed higher SP in HpSp compared to LP. The primary motor cortex showed no differences, but the visual cortex showed higher SP in LP compared with typical AD.

Normalized hippocampal area, neuronal density of the CA1-subiculum, and ratio of the CA1-subiculum to fusiform gyrus thickness for each type are shown in **Table 2**. HpSp cases had higher structural measurements compared with both typical AD and LP, which also differed from each other. Each structural variable inversely associated with CA1-subiculum NFT ($p<0.0001$).

Table 3 shows the results of *MAPT* genotype differences between the three AD subtypes. There was a significant over-representation of H1H1 homozygotes in LP compared to HpSp. Given that Lewy body pathology is more frequent in LP than in HpSp and that *MAPT* has been shown to be a risk factor for Parkinson's disease,[29] a multiple logistic regression was performed to control for Lewy body pathology. This showed that the effect was independent of Lewy body pathology [odds ratio for H1H1 was 2.99 ($p = 0.003$) for LP compared to HpSp] (**Supplemental Table 4**). There were no allele effects for *APOE* by AD subtype. *APOE* genotype differences were found between HpSp and LP with a higher proportion of ε4 non-carriers approaching significance in the HpSp (50%) versus LP (38%) ($p = 0.067$). To investigate the hypothesis that *APOE* allele frequency is associated with age of onset in AD as recently suggested by Scheltens, et al.,[30] AD was stratified as early-onset or late-onset using 65 years as the cutoff. **Table 3** shows that HpSp is equally represented across the four classes, but LP was over-represented in the late onset/ε4+ class. This finding suggests that *APOE* has more impact on LP and typical AD than HpSp. In accord with this, *APOE* ε4 carriers had smaller hippocampal area ($p=0.028$), fewer neurons ($p=0.004$), and higher hippocampal NFT counts ($p<0.001$) than non-carriers. There was no difference in *SNCA* genotype or family history of neurodegenerative disease amongst the AD subtypes.

Clinical findings are summarized in **Table 1**. Age of onset was less in HpSp and greater in LP compared to typical AD. HpSp had a shorter disease duration, but there was no significant difference between LP and typical AD. A non-AD clinical diagnosis was more frequent (30%) in HpSp than LP and typical AD. Examples of non-AD clinical diagnoses included behavioral variant of frontotemporal dementia (12%) and other focal cortical syndromes (13%), such as progressive nonfluent aphasia, semantic dementia, posterior cortical syndrome, and corticobasal syndrome, as well as parkinsonian disorders (4%), such as progressive supranuclear palsy and Parkinson's disease dementia. In contrast, LP most often had an antemortem clinical diagnosis of AD (94%). Of the 6% of LP who were given a non-AD clinical diagnosis, only a few were considered to have behavioral variant of frontotemporal dementia ($n=2$) or focal cortical syndromes ($n=1$), but they were comparable on parkinsonian diagnoses ($n=4$). This finding remained significant regardless of whether the cases came from a non-AD study center (**Supplemental Table 3**). Neither initial, nor final MMSE scores assessed within three years of onset and death, respectively, were different among the AD types. When MMSE scores were evaluated with respect to disease duration, apparent differences were observed for HpSp. **Figure 4** shows rapid progression of

deterioration on MMSE in HpSp, with many patients progressing from normal to impaired values in a few years, declining at a rate of 5 points per year on the MMSE. On average, HpSp cases showed a steeper slope than both LP and typical AD. LP cases showed a more gradual decline of 1 point per year compared to typical AD, which declined at a rate of 3 points per year. Age at onset likely plays a confounding role in comparison of cognitive decline between the three AD subtypes, and larger longitudinal series are needed to better evaluate this.

Hippocampal and cortical NFT densities were correlated with disease duration in typical AD ($r = 0.47$, $p < 0.001$ and $r = 0.44$, $P < 0.001$, respectively). LP cases showed a weak inverse association between CA1-subicular neuronal density and disease duration ($r = -0.20$, $p = 0.086$) and no relationship with age of onset. Subiculum ($r = 0.28$, $p = 0.014$) and mid-frontal NFT density ($r = 0.29$, $p = 0.012$) positively correlated with disease duration, but no relationship was found with CA1, inferior parietal, or superior temporal NFT density in LP cases. Neither disease duration nor age of onset associated with CA1-subicular neuronal density in HpSp cases. To add further evidence of the uniqueness of HpSp subtype, the only relationship between disease duration and NFT density was in the mid-frontal cortex ($r = 0.24$, $p = 0.043$).

Replication cohort

Supplemental Table 5 shows the summary of clinical, demographic and pathologic characteristics of the replication cohort, obtained from AD patients from a community-based prospective longitudinal study. The replication series (mean = 86 years) was older at death compared to the original cohort (mean = 79 years), but showed the same relationships between age at death and AD subtypes, with HpSp being youngest of the three ($p < 0.001$). We interpret the higher proportion of LP (21%) compared with HpSp (9%) in this cohort to be related to the older age of the community-based cohort compared with the initial cohort. Similar to the initial cohort, the HpSp cases had lower hippocampal NFT and higher NFT counts in the three association cortices than both LP and typical AD (all $p < 0.001$). Conversely, LP had lower cortical NFT and higher hippocampal NFT than both HpSp and typical AD (all $p < 0.001$). Age of onset was lower in HpSp than both LP and typical AD ($p = 0.007$). An atypical clinical diagnosis was more frequent in HpSp compared to LP and typical AD, with no LP cases having been misdiagnosed (all $p<0.001$). The rate of longitudinal decline in MMSE scores was also replicated, with fastest rate in HpSp and the slowest in LP ($p = 0.040$).

Discussion

Using quantitative methods of measuring neurofibrillary tangle burden to classify AD, it was possible to identify pathologic, demographic, structural, genetic, and clinical differences between typical and atypical AD. The latter was composed of two distinct subtypes – hippocampal sparing AD and limbic predominant AD. HpSp cases were younger at death and more often male. An operationally-defined algorithm sorted the HpSp cases from the AD population by evaluating NFT counts in hippocampus and association cortices. Hippocampal regions not included in the algorithm were independently shown to be spared. Unexpectedly, HpSp cases had higher NFT densities in association cortices, as well as the motor cortex. Not surprisingly, these cases had larger hippocampi, as well as higher neuronal counts in the CA1-subiclum. The H1H1 *MAPT* genotype was underrepresented in HpSp. When age was taken into account, early-onset ε4 carriers were more likely to be HpSp and late-onset ε4 carriers were more likely to be LP or typical AD. Clinically, HpSp cases had distinctive features, including earlier onset, shorter disease duration, rapid progression and more often focal cortical clinical syndromes such as behavioral variant frontotemporal dementia, progressive aphasia or posterior cortical syndrome. The salient

findings were confirmed in an independent cohort of AD patients derived from a single center in which patients were enrolled in a prospective longitudinal study.

The clinical, genetic and pathological findings support the hypothesis that a significant number of AD cases (about 25%) do not conform to typical AD. A recent report comes to a similar conclusion based upon analysis of only *APOE* ε4 allele status and age at onset.[30] Using quantitative neuropathologic features, in particular, differential anatomical distributions of neurofibrillary degeneration, we classified AD into three distinct subtypes. The implication of AD subtypes on neuroimaging hippocampal volume studies warrants attention. The hippocampal volume discernment between controls, mild cognitive impairment and AD has been consistently found; however, variability observed in antemortem hippocampal changes associated with AD may in part be related to heterogeneity of AD.[1, 2, 4, 31] Of particular interest is a recent voxel-based morphometric study that showed evidence of atypical AD that had imaging characteristics that would fit with HpSp as defined in the present study. In particular, they had temporoparietal atrophy, but lack of hippocampal volume loss compared to typical AD.[13] Taken together with the present findings, it is possible that HpSp cases dilute the sensitivity and specificity in hippocampal volumetric studies in AD. Conversely, LP cases may exaggerate hippocampal atrophy, but may blunt the effect on associations between hippocampal size and cognitive decline owing to their later age of onset and longer and slower disease course.

In the present study, no AD patients were included that also had hippocampal sclerosis, as defined by neuronal loss and gliosis in the hippocampal CA1 and subicular subfields disproportionate to NFTs.[32, 33] This was done to avoid contamination of the classification algorithm by cases with low NFT counts due to neuronal loss, which might artificially appear to have HpSp. Hippocampal sclerosis tends to be increasingly common with advanced age,[32, 33] and to be associated with TDP-43 pathology in 70% to 90% of cases.[23, 33] In contrast, TDP-43 pathology was uncommon in HpSp (13%), which was also associated with younger age. TDP-43 pathology is detected in 30% to 60% of AD cases,[23, 34] and TDP-43 inclusions are within neurons with NFT in some cases.[23] In the present series, 30% of typical AD and LP cases had TDP-43 pathology, which fits with evidence from other studies that TDP-43 pathology is more frequent in AD with severe limbic neurofibrillary pathology and is associated with medial temporal atrophy with voxel-based morphometry.[35]

LP cases share several similarities with a previously described subset of late onset dementia cases, termed limbic neurofibrillary tangle dementia[36] or more commonly, tangle predominant dementia.[37, 38] LP and tangle predominant dementia are more frequent in women and both conditions are associated with a higher age of death compared to typical AD. NFT in tangle predominant dementia are typically limited to allocortical regions with few isocortical NFT, similar to LP. The major difference between the LP and tangle predominant dementia is the extent of SPs. Table 2 shows that not only are SPs present in LP cases, there is little difference in density of SP between the other two AD subtypes. This could in part be methodological, with thioflavin-S fluorescent microscopy detecting a wide range of plaque types, including nonneuritic diffuse amyloid deposits, which make up the bulk of cortical amyloid deposits in tangle predominant dementia when SP are present.[39] LP cases had a higher frequency of the *APOE* ε4 allele when adjusting for old age, whereas the ε2 and ε3 alleles have been reported to be increased in tangle predominant dementia regardless of age.[40] A shorter disease duration of 5 years has been reported for tangle predominant dementia compared to the much longer 10 years disease duration we observed in LP cases.[37] Although cognitive impairment is similarly less impaired, it is our contention that LP is a subtype of atypical AD that should be considered in research studies and clinical trials and not necessarily tangle predominant dementia.

The widely-used Braak neurofibrillary tangle staging scheme posits that the nidus of Alzheimer neurofibrillary degeneration is the transentorhinal cortex, with subsequent extension into layer II neurons of the entorhinal cortex and then the hippocampus.[7] The present study provides evidence that "spread" from transentorhinal/hippocampal area may not be the only pattern of pathologic progression in AD. Previous reports have shown that NFT correlate with disease duration, supporting the idea of a progressive accumulation of tau pathology.[10, 41] The typical AD cases in this study similarly show a positive relationship with disease duration and NFT in both the hippocampus and cortex. A relationship was found in the LP cases between disease duration and NFT in the hippocampus, while middle frontal gyrus NFT correlated with disease duration in HpSp cases, suggesting that the origin and "spread" of the disease process may differ substantially between these two extreme AD subtypes.

The observed correlation between disease duration and frontal NFT in HpSp suggests that in this AD subtype cortical neurons are selectively vulnerable, while hippocampal neurons are relatively resistant. This pattern of selective vulnerability may explain the disproportionate number of cases with focal clinical presentations (*e.g.*, behavioral variant frontotemporal dementia, primary progressive aphasia and posterior cortical syndrome) in HpSp. Focal cortical pathology has been previously described in a subset of AD cases with atypical presentations, including posterior cortical syndrome, some of which had HpSp.[42] The present findings emphasize the importance of considering atypical AD (with HpSp) in the differential diagnosis of focal cortical syndromes, especially in younger men.

There are inherent limitations in retrospective studies such as the present discovery cohort, but similar findings in a smaller prospective longitudinal replication cohort suggest that the findings in the discovery cohort have inherent validity. Given the retrospective nature of the present study, it was only possible to assess cognitive status with widely used clinical measures (*e.g.*, MMSE) to track differences in disease progression in the AD subtypes. It must be emphasized that the results of longitudinal studies of MMSE reported herein are considered exploratory at this time. Future studies are needed in prospective longitudinal cohorts, in which more sensitive and comprehensive cognitive testing is available, to further define the clinical and neuropsychological characteristics of AD subtypes.

A significant strength of the present study is the large sample size and the presence of quantitative data collected by a single observer using a simple, sensitive and highly reproducible method, thioflavin S fluorescent microscopy. AD subtypes were objectively defined by a mathematical algorithm, but HpSp and LP subtypes, at least in their extreme expressions, can readily be identified using qualitative assessments by a skilled observer, although formal verification and assessment of interrater reliability remains an important future objective. While thioflavin S fluorescent microscopy is a very sensitive method for detecting Alzheimer type tangles, it like other similar fluorochromes (*e.g.*, thiazin red) is not a suitable method for all types of neurofibrillary pathology.[43] It does not recognize tangles in non-Alzheimer tauopathies, and it does not recognize so-called "pretangles;" although, it is currently unclear if these have clinical significance in AD. Thioflavin-S is an excellent method for detecting the amyloid component of SP, but it is often more difficult to differentiate subtypes of SP. A future study should address AD subtypes using amyloid and tau immunohistochemistry.

Pathologic classification of AD subtypes with distinct clinical presentations point to the need of further research into the nature of the initiation and progression of tau pathology in atypical AD and the need to consider atypical presentations in prospective, longitudinal studies of dementia. In addition, the existence of distinct clinical and pathologic subtypes of AD should be considered in designing and interpreting biomarker studies.

Supplementary Material

Refer to Web version on PubMed Central for supplementary material.

Acknowledgments

The project was supported by the Mayo ADRC grant (P50 AG16574), Mayo Clinic Study on Aging (*aka* ADPR; U01 AG06786), Florida ADRC (P50 AG215711), Einstein Aging Study (P01 AG03949), Florida Alzheimer's Disease Initiative and NIH funding from Jennifer L. Whitwell, PhD (R21 AG038736). OAR and DWD are supported by the Mayo Clinic Udall Center (P50 NS072187). The funding sources had no role in study design, collection, analysis, interpretation, or decision to submit this paper. We thank the patients and their families who have donated brains to help further our knowledge in neurodegeneration. The authors would like to acknowledge the endless hours of commitment and teamwork offered by Linda G. Rousseau, Virginia R. Phillips, John Gonzalez, and Monica Castanedes-Casey. We would like to thank Jennifer Whitwell, Kris Johnson, and Jeremiah Aakre for assistance in collection of data and pathologic material for the replication cohort.

References

1. Jack CR Jr. Petersen RC, Xu Y, O'Brien PC, Smith GE, Ivnik RJ, et al. Rate of medial temporal lobe atrophy in typical aging and Alzheimer's disease. Neurology. 1998; 51(4):993–9. [PubMed: 9781519]
2. De Leon MJ, George AE, Golomb J, Tarshish C, Convit A, Kluger A, et al. Frequency of hippocampal formation atrophy in normal aging and Alzheimer's disease. Neurobiol Aging. 1997; 18(1):1–11. [PubMed: 8983027]
3. Desikan RS, Sabuncu MR, Schmansky NJ, Reuter M, Cabral HJ, Hess CP, et al. Selective disruption of the cerebral neocortex in Alzheimer's disease. PLoS One. 2010; 5(9):e12853. [PubMed: 20886094]
4. Frisoni GB, Ganzola R, Canu E, Rub U, Pizzini FB, Alessandrini F, et al. Mapping local hippocampal changes in Alzheimer's disease and normal ageing with MRI at 3 Tesla. Brain. 2008; 131(Pt 12):3266–76. [PubMed: 18988639]
5. Jack CR Jr, Knopman DS, Jagust WJ, Shaw LM, Aisen PS, Weiner MW, et al. Hypothetical model of dynamic biomarkers of the Alzheimer's pathological cascade. The Lancet Neurology. 2010; 9(1): 119–28.
6. Giannakopoulos P, Hof PR, Bouras C. Alzheimer's disease with asymmetric atrophy of the cerebral hemispheres: morphometric analysis of four cases. Acta Neuropathol. 1994; 88(5):440–7. [PubMed: 7847073]
7. Braak H, Braak E. Neuropathological stageing of Alzheimer-related changes. Acta Neuropathol. 1991; 82(4):239–59. [PubMed: 1759558]
8. Hyman BT, Trojanowski JQ. Consensus recommendations for the postmortem diagnosis of Alzheimer disease from the National Institute on Aging and the Reagan Institute Working Group on diagnostic criteria for the neuropathological assessment of Alzheimer disease. J Neuropathol Exp Neurol. 1997; 56(10):1095–7. [PubMed: 9329452]
9. Arnold SE, Hyman BT, Flory J, Damasio AR, Van Hoesen GW. The Topographical and Neuroanatomical Distribution of Neurofibrillary Tangles and Neuritic Plaques in the Cerebral Cortex of Patients with Alzheimer's Disease. Cerebral Cortex. 1991; 1(1):103–16. [PubMed: 1822725]
10. Arriagada PV, Growdon JH, Hedley-Whyte ET, Hyman BT. Neurofibrillary tangles but not senile plaques parallel duration and severity of Alzheimer's disease. Neurology. 1992; 42(3):631. [PubMed: 1549228]
11. Vemuri P, Wiste HJ, Weigand SD, Knopman DS, Trojanowski JQ, Shaw LM, et al. Serial MRI and CSF biomarkers in normal aging, MCI, and AD. Neurology. 2010; 75(2):143–51. [PubMed: 20625167]
12. Hof PR, Bouras C, Constantinidis J, Morrison JH. Balint's syndrome in Alzheimer's disease: specific disruption of the occipito-parietal visual pathway. Brain Res. 1989; 493(2):368–75. [PubMed: 2765903]

13. Whitwell JL, Jack CR Jr. Przybelski SA, Parisi JE, Senjem ML, Boeve BF, et al. Temporoparietal atrophy: A marker of AD pathology independent of clinical diagnosis. Neurobiol Aging. 2009
14. Dickson DW, Crystal H, Mattiace LA, Kress Y, Schwagerl A, Ksiezak-Reding H, et al. Diffuse Lewy body disease: light and electron microscopic immunocytochemistry of senile plaques. Acta Neuropathol. 1989; 78(6):572–84. [PubMed: 2683563]
15. Nelson PT, Abner EL, Schmitt FA, Kryscio RJ, Jicha GA, Santacruz K, et al. Brains with medial temporal lobe neurofibrillary tangles but no neuritic amyloid plaques are a diagnostic dilemma but may have pathogenetic aspects distinct from Alzheimer disease. J Neuropathol Exp Neurol. 2009; 68(7):774–84. [PubMed: 19535994]
16. Barker WW, Luis CA, Kashuba A, Luis M, Harwood DG, Loewenstein D, et al. Relative frequencies of Alzheimer disease, Lewy body, vascular and frontotemporal dementia, and hippocampal sclerosis in the State of Florida Brain Bank. Alzheimer Dis Assoc Disord. 2002; 16(4):203–12. [PubMed: 12468894]
17. Uchikado H, Lin WL, DeLucia MW, Dickson DW. Alzheimer disease with amygdala Lewy bodies: a distinct form of alpha-synucleinopathy. J Neuropathol Exp Neurol. 2006; 65(7):685–97. [PubMed: 16825955]
18. Togo T, Sahara N, Yen SH, Cookson N, Ishizawa T, Hutton M, et al. Argyrophilic grain disease is a sporadic 4-repeat tauopathy. J Neuropathol Exp Neurol. 2002; 61(6):547–56. [PubMed: 12071638]
19. Terry RD, Hansen LA, DeTeresa R, Davies P, Tobias H, Katzman R. Senile dementia of the Alzheimer type without neocortical neurofibrillary tangles. J Neuropathol Exp Neurol. 1987; 46(3):262–8. [PubMed: 2881985]
20. Khachaturian ZS. Diagnosis of Alzheimer's disease. Arch Neurol. 1985; 42(11):1097–105. [PubMed: 2864910]
21. Jellinger KA, Attems J. Incidence of cerebrovascular lesions in Alzheimer's disease: a postmortem study. Acta Neuropathol. 2003; 105(1):14–7. [PubMed: 12471455]
22. Fujishiro H, Ferman TJ, Boeve BF, Smith GE, Graff-Radford NR, Uitti RJ, et al. Validation of the neuropathologic criteria of the third consortium for dementia with Lewy bodies for prospectively diagnosed cases. J Neuropathol Exp Neurol. 2008; 67(7):649–56. [PubMed: 18596548]
23. Amador-Ortiz C, Lin WL, Ahmed Z, Personett D, Davies P, Duara R, et al. TDP-43 immunoreactivity in hippocampal sclerosis and Alzheimer's disease. Ann Neurol. 2007; 61(5): 435–45. [PubMed: 17469117]
24. Folstein MF, Folstein SE, McHugh PR. “Mini-mental state”. A practical method for grading the cognitive state of patients for the clinician. J Psychiatr Res. 1975; 12(3):189–98. [PubMed: 1202204]
25. Duvernoy, HM. The human hippocampus : an atlas of applied anatomy. J.F. Bergmann; München: 1988.
26. Baker M, Litvan I, Houlden H, Adamson J, Dickson D, Perez-Tur J, et al. Association of an extended haplotype in the tau gene with progressive supranuclear palsy. Hum Mol Genet. 1999; 8(4):711–5. [PubMed: 10072441]
27. Crook R, Hardy J, Duff K. Single-day apolipoprotein E genotyping. J Neurosci Methods. 1994; 53(2):125–7. [PubMed: 7823614]
28. Ross OA, Gosal D, Stone JT, Lincoln SJ, Heckman MG, Irvine GB, et al. Familial genes in sporadic disease: common variants of alpha-synuclein gene associate with Parkinson's disease. Mech Ageing Dev. 2007; 128(5-6):378–82. [PubMed: 17531291]
29. Zabetian CP, Hutter CM, Factor SA, Nutt JG, Higgins DS, Griffith A, et al. Association analysis of MAPT H1 haplotype and subhaplotypes in Parkinson's disease. Ann Neurol. 2007; 62(2):137–44. [PubMed: 17514749]
30. van der Flier WM, Pijnenburg YAL, Fox NC, Scheltens P. Early-onset versus late-onset Alzheimer's disease: the case of the missing APOE ε4 allele. The Lancet Neurology. 2011; 10(3): 280–8.
31. Craig-Schapiro R, Fagan AM, Holtzman DM. Biomarkers of Alzheimer's disease. Neurobiol Dis. 2009; 35(2):128–40. [PubMed: 19010417]

32. Dickson DW, Davies P, Bevona C, Van Hoeven KH, Factor SM, Grober E, et al. Hippocampal sclerosis: a common pathological feature of dementia in very old (> or = 80 years of age) humans. Acta Neuropathol. 1994; 88(3):212–21. [PubMed: 7810292]
33. Nelson PT, Schmitt FA, Lin Y, Abner EL, Jicha GA, Patel E, et al. Hippocampal sclerosis in advanced age: clinical and pathological features. Brain. 2011; 134(Pt 5):1506–18. [PubMed: 21596774]
34. Arai T, Mackenzie IR, Hasegawa M, Nonoka T, Niizato K, Tsuchiya K, et al. Phosphorylated TDP-43 in Alzheimer's disease and dementia with Lewy bodies. Acta Neuropathol. 2009; 117(2): 125–36. [PubMed: 19139911]
35. Josephs KA, Whitwell JL, Knopman DS, Hu WT, Stroh DA, Baker M, et al. Abnormal TDP-43 immunoreactivity in AD modifies clinicopathologic and radiologic phenotype. Neurology. 2008; 70(19 Pt 2):1850–7. [PubMed: 18401022]
36. Iseki E, Yamamoto R, Murayama N, Minegishi M, Togo T, Katsuse O, et al. Immunohistochemical investigation of neurofibrillary tangles and their tau isoforms in brains of limbic neurofibrillary tangle dementia. Neuroscience Letters. 2006; 405(1-2):29–33. [PubMed: 16859829]
37. Jellinger KA, Attems J. Neurofibrillary tangle-predominant dementia: comparison with classical Alzheimer disease. Acta Neuropathol. 2007; 113(2):107–17. [PubMed: 17089134]
38. Jellinger KA, Bancher C. Senile dementia with tangles (tangle predominant form of senile dementia). Brain Pathol. 1998; 8(2):367–76. [PubMed: 9546293]
39. Braak H, Braak E. Neurofibrillary changes confined to the entorhinal region and an abundance of cortical amyloid in cases of presenile and senile dementia. Acta Neuropathol. 1990; 80(5):479–86. [PubMed: 2251904]
40. Bancher C, Egensperger R, Kosel S, Jellinger K, Graeber MB. Low prevalence of apolipoprotein E epsilon 4 allele in the neurofibrillary tangle predominant form of senile dementia. Acta Neuropathol. 1997; 94(5):403–9. [PubMed: 9386771]
41. Kril J, Patel S, Harding A, Halliday G. Neuron loss from the hippocampus of Alzheimer's disease exceeds extracellular neurofibrillary tangle formation. Acta Neuropathologica. 2002; 103(4):370–6. [PubMed: 11904757]
42. Tang-Wai DF, Graff-Radford NR, Boeve BF, Dickson DW, Parisi JE, Crook R, et al. Clinical, genetic, and neuropathologic characteristics of posterior cortical atrophy. Neurology. 2004; 63(7): 1168–74. [PubMed: 15477533]
43. Uchihara T, Nakamura A, Yamazaki M, Mori O. Evolution from pretangle neurons to neurofibrillary tangles monitored by thiazin red combined with Gallyas method and double immunofluorescence. Acta Neuropathol. 2001; 101(6):535–9. [PubMed: 11515780]

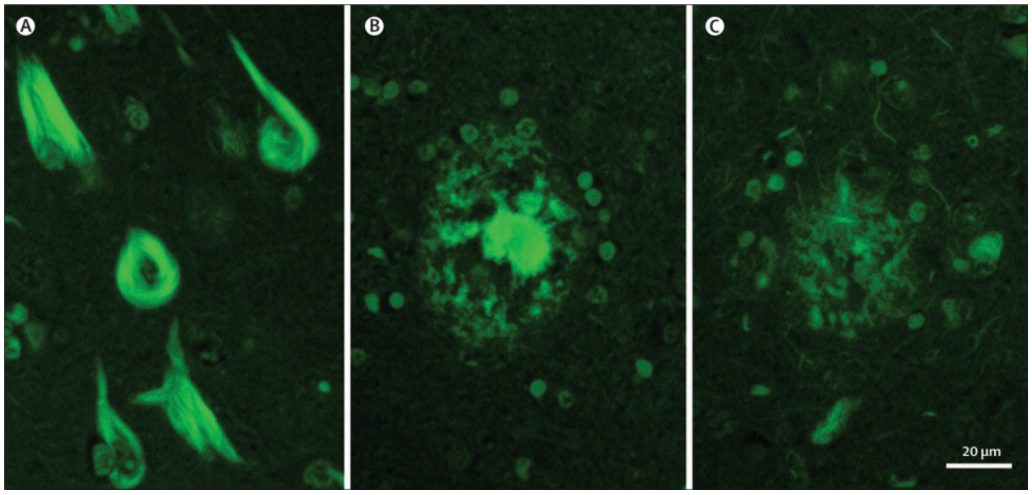

Figure 1.
Photomicrograph of thioflavin S fluorescent microscopic images of neurofibrillary tangles (A), used in the operational classification algorithm, and of senile plaques with dense core (B) or neuritic elements (C). Magnification bar = 20 µm.

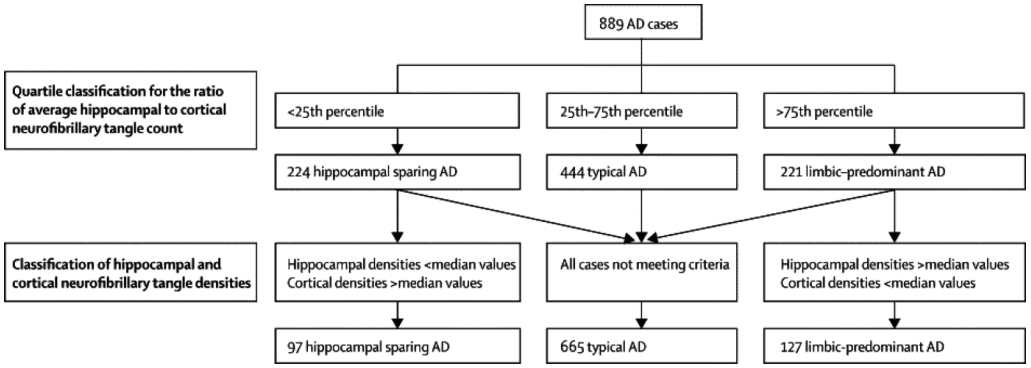

Figure 2.

This diagram demonstrates the classification system used by the algorithm (dotted lines) and the resultant sample size of each subtype (solid line). The ratio between the hippocampal and cortical NFT was used to determine the cases with relative sparing of the hippocampus or cortex, however, this would have only classified cases in the 25th and 75th quartiles. By using NFT median counts, regional pathology and over/underestimation of these regional differences could be used to further differentiate the groups. The resultant asymmetry in the sample population of AD subtypes is a product of the differences in each of the hippocampal (i.e. CA1 and subiculum) and cortical areas (i.e. superior temporal, inferior parietal, and mid-frontal) individually evaluated.

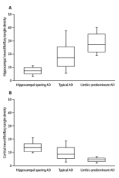

Figure 3.

The CA1 and subiculum of the posterior hippocampus and three association cortices were sampled, stained with Thioflavin-S, and reviewed at x400 to obtain neurofibrillary tangle counts. An algorithm was developed to operationally define relative hippocampal sparing AD, typical AD, and limbic predominant AD. These cases were analyzed for differences in averaged hippocampal **(A)** and cortical NFT counts **(B).** The HpSp group had a higher cortical density than both typical and limbic predominant AD. Converesly, limbic predominant AD had higher hippocampal NFT compared to typical and HpSp AD.

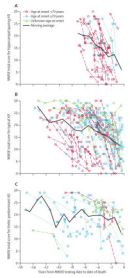

Figure 4.

Longitudinal progression of cognitive decline in hippocampal sparing **(A)**, typical **(B)**, and limbic predominant AD **(C)** differs greatly amongst the groups with regard to MMSE total score. Age of onset was stratified in each graph according to the discovery set's median age at disease onset [<70 years (red) and ≥70 years (blue)]. A moving average was plotted to illustrate overall longitudinal decline in MMSE for each of the three AD subtypes.

Table 1

Subject characteristics

Characteristic	AD subtypes HpSp	Typical	LP	Statistics *p*	(stat test)
Number (% total of n=889)	97 (11%)	665 (75%)	127 (14%)		
Age, mean yr. (SD)	73 (10)	79 (9)	86 (6)	<0.001	(ANOVA)[a,b,c]
Females (% total of AD type)	36 (37%)	368 (55%)	87 (69%)	<0.001	(chi-square)[a,b,i]
Education, mean yr. (SD)	15 (3)	14 (3)	14 (3)	0.139	(ANOVA)
Postmortem findings					
Brain weight, mean g. (SD)	1054 (120)	1040 (158)	1043 (127)	0.686	(ANOVA)
NFT Braak stage, median (IQR)	6 (5.0,6.0)	6 (5.0,6.0)	5.5 (5.0,6.0)	0.096	(ANOVA on ranks)
Other pathologic processes/total (% total of AD type)					
TDP-43+	13/97 (13%)	170/559 (30%)	30/100 (30%)	0.002	(chi-square)[a,e]
Vascular disease	16/97 (16%)	184/665 (28%)	46/127 (36%)	0.005	(chi-square)[g,e]
Lewy body disease	11/97 (11%)	172/665 (26%)	33/127 (26%)	0.007	(chi-square)[d,e]
Clinical findings*					
Age of onset, mean yr. (SD)	63 (10)	69 (10)	76 (7)	<0.001	(ANOVA)[a,b,c]
Disease duration, mean yr. (SD)	8 (3)	9 (4)	10 (4)	0.009	(ANOVA)[a,b]
Atypical clinical/Total (% total of AD type)	27/91 (30%)	102/606 (17%)	7/113 (6%)	<0.001	(chi-square)[d,b,f]
MMSE					
Initial score, median (IQR)*	20 (15,25)	23 (15,26)	23 (18,28)	0.64	(ANOVA on ranks)
Final score, median (IQR)*	7 (2,13)	11 (6,16)	15 (8,19)	0.076	(ANOVA on ranks)[h]
Longitudinal decline (IQR)*	-4.8 (-8.3,-3.1)	-2.8 (-4.4,-1.5)	-1.4 (-2.8,-0.8)	0.009	(ANOVA on ranks)[g,e,i]

Acronyms: HpSp – hippocampal sparing (HS), Typical – classic progression of AD from limbic regions to cortex (T), LP – limbic predominant (LP), SD – standard deviation, IQR – interquartile range, ANOVA – analysis of variance; Total refers to the number of cases evaluated out of the group. Pairwise comparisons (means: t-test, medians: Mann-Whitney rank sum test):

[a] p≤0.001 HS vs. T

[b] p≤0.001 HS vs. LP

[c] p≤0.001 T vs. LP

[d] p≤0.01 HS vs. T

[e] p≤0.01 HS vs. LP

[f] p≤0.01 T vs. LP

[g] p<0.05 HS vs. T

[h] p<0.05 HS vs. LP

[i] p<0.05 T vs. LP.

[*] Median MMSE score assessed within 3 years of symptom onset (initial) or death (final). After clinical history was reviewed, a subset of cases had clinical data available for HpSp (n=97), Typical (n=232), and LP (n=127): age of onset (73/203/77), education (71/214/90), MMSE ≥1 visit (43/160/46), and longitudinal MMSE ≥3 visits (18/52/18).

Table 2

Quantitative pathology

Characteristic	HpSp	AD subtypes Typical	LP	Statistics *p*-value[a]
Neurofibrillary tangle counts				
Algorithm-based regions *				
CA1	5 (4,8)	13 (8,20)	18 (14,26)	<0.001[b]
Subiculum	8 (5,12)	20 (11,33)	35 (28,45)	<0.001[b]
Superior temporal	15 (12,20)	12 (6,17)	6 (4,9)	<0.001[b]
Inferior parietal	14 (11,20)	8 (4,14)	4 (2,5)	<0.001[b]
Mid-frontal	11 (7,14)	5 (2,12)	2 (1,3)	<0.001[b]
Independent regions				
Amygdala, lateral	6 (3,6)	8 (4,13)	9 (6,13)	0.002[e,f]
Amygdala, medial	12 (6,20)	17 (8,30)	23 (16,31)	<0.001[d,f,h]
CA2/3	2 (1,4)	5 (2,9)	5 (3,10)	<0.001[c]
Endplate	2 (1,3)	3 (2,5)	3 (2,5)	<0.001[c]
Visual cortex	1 (0,3)	1 (0,4)	1 (0,2)	0.138
Motor cortex	1 (1,2)	1 (0,2)	0 (0,1)	<0.001[b]
Senile plaque counts				
CA1	9 (5,13)	9 (5,15)	7 (4,14)	0.223
CA2/3	2(1,5)	2 (0,4)	2 (0,3)	0.053[g]
Endplate	2 (1,8)	4 (1,8)	3 (1,8)	0.428
Subiculum	18 (11,31)	21 (14,32)	22 (14,33)	0.135
Motor cortex	24 (15,35)	24 (15,35)	21 (15,30)	0.177
Visual cortex	33 (22,46)	38 (24,50)	30 (20,46)	0.007[h]
Structural differences				
Hipp. Area/Brain weight, cm^2/g	440 (360,500)	370 (320,430)	330(290,370)	<0.001[b]
CAI-Subiculum neurons/mm^2	140 (110,150)	120 (90,140)	100 (80,120)	<0.001[b]
CA1 -Subiculum/Fusiform	0.68 (0.56,0.83)	0.53 (0.41,0.69)	0.40 (0.32,0.53)	<0.001[b]

All values shown as median (IQR);

[a] Kruskal-Wallis One Way Analysis of Variance on Ranks, IQR – 25%-75% interquartile range; Mann-Whitney rank sum test yielded

[b] p<0.001

[c] p<0.02 for each comparison between AD subtypes;

[d] p<0.001

[e] p<0.01 between HpSp vs. typical

[f] $p<0.001$

[g] $p<0.05$ between HpSp vs. LP

[h] $p<0.01$ between typical vs. LP.

[*] Regions used to operationally define AD types.

Table 3

MAPT genotyping

MAPT	**H1H1**	**non-H1H1**		**EOAD/e4-**	**EOAD/e4+**	**LOAD/e4-**	**LOAD/e4+**	
Hippocampal sparing	24 (46%)	28 (54%)	χ^2; p = 0.024[a]	10 (29%)	8 (24%)	8 (24%)	8 (24%)	χ^2; p < 0.001
Typical	204 (59%)	139 (41%)		4 (7%)	10 (19%)	18 (33%)	22 (41%)	
Limbic Predominant	54 (70%)	23 (30%)		1 (2%)	3 (6%)	13 (27%)	32 (65%)	

Acronyms: MAPT – microtubule associated protein – Tau, non-H1 H1 – H1H2 & H2H2, EOAD – early onset AD requires age of onset < 65 years old, LOAD – late onset AD requires age of onset ≥ 65

[a] *MAPT* chi-square test yielded p<0.01 between HpSp and LP.